MULTI-SCALE WAVELET AND DEEP LEARNING INTEGRATED ADAPTIVE WEIGHTED NON-LOCAL MEANS DENOISING ALGORITHM

by

Hongjin MA[a*], Jiayu ZHAO[a], and Weiwei ZHANG[b]

[a]School of Science, Xi'an University of Architecture and Technology, Xi'an, China
[b]School of Mathematics and Statistics, Northwestern Polytechnical University, Xi'an, China

Original scientific paper
https://doi.org/10.2298/TSCI2602251M

Image denoising is a critical component in numerous disciplines, including medical imaging, remote sensing, and computer vision. This paper presents an adaptive weighted non-local means (MAW-NLM) algorithm, which employs multi-scale wavelet decomposition and deep learning to address the shortcomings of conventional non-local means in more intricate scenarios. The initial step in the image decomposition process involves the division of the image into low- and high-frequency components through the implementation of multi-scale wavelet decomposition. This decomposition is followed by the processing of each component individually, with the objective of preserving edges and fine details with greater efficacy. A deep learning-based similarity metric, leveraging a convolutional neural network for high-dimensional feature extraction, replaces the conventional Euclidean distance, thus enhancing the robustness of the similarity measurement. Furthermore, the algorithm dynamically adjusts smoothing parameters based on local gradient and texture complexity, significantly improving its adaptability. The integration of a fast nearest-neighbor search algorithm and a two-stage optimization approach has been demonstrated to enhance both computational efficiency and denoising effectiveness. The experimental results demonstrate the superiority of MAW-NLM in comparison to traditional methods.

Key words: *image denoising, non-local means, multi-scale wavelet, deep learning, adaptive smoothing*

Introduction

Image denoising is a critical component of image processing, with applications spanning domains such as medical imaging, remote sensing, and computer vision. The presence of noise in images can substantially compromise their quality, hindering further analysis. Consequently, the development of efficient denoising algorithms is imperative for enhancing image quality and enabling accurate downstream tasks.

Conventional techniques, including Gaussian and median filtering, frequently encounter difficulties in preserving fine details such as edges and textures while reducing noise. The non-local mean (NLM) algorithm, as proposed by Buades *et al.* [1], has been shown to effectively address this issue by averaging similar patches across the image. This approach has been demonstrated to preserve edges while reducing noise, thereby enhancing the clarity

* Corresponding author, e-mail: hjma@xauat.edu.cn

and detail of the image. While NLM has proven to be an effective tool, it does face challenges with computational efficiency and adaptability, especially in complex scenarios such as medical or high-texture images.

To enhance NLM, a series of modifications have been put forth. Guo *et al.* [2] applied the NLM algorithm to infrared image denoising, highlighting its domain-specific effectiveness. Other methodologies, such as 3-D Filtering by Block Matching and Convolutional Neural Network [3], employ a combination of spatial-domain and transform-domain techniques to enhance denoising, particularly in the context of medical imaging [4, 5].

The advent of deep learning [6, 7] has precipitated substantial progress in the domain of image denoising. In their seminal work, Zhang *et al.* [8] proposed a deep residual learning framework that utilizes convolutional neural networks (CNN). This framework has been shown to outperform traditional methods by learning residuals of noisy images. Additionally, FFDNet introduced a fast and flexible CNN-based denoising method, offering real-time computational efficiency [9].

Deep learning methods, including U-Net for biomedical image segmentation [10] and MemNet for image restoration [11], have demonstrated efficacy in preserving details while denoising. Lefkimmiatis [12] applied convolutional neural networks (CNN) to the denoising of color images, achieving a substantial enhancement in quality. Zhang *et al.* [13] proposed an adaptive unsupervised deep learning denoising method for medical imaging with unbiased estimation and Hessian-based regularization.

Despite the apparent success of deep learning methodologies, the balancing of performance and computational efficiency remains a significant challenge. The proposed methodology integrates a hybrid approach, integrating multi-scale wavelet decomposition with deep learning-based similarity measures. This integration aims to enhance denoising performance while maintaining computational efficiency.

The traditional NLM algorithm can be expressed mathematically:

$$I_{\text{denoised}}(x) = \frac{\sum_{y \in \Omega} w(x,y) I(y)}{\sum_{y \in \Omega} w(x,y)}$$

where $I(x)$ is the noisy image, $w(x, y)$ – the weight function, and Ω – the search window.

Method

The proposed MAW-NLM algorithm is comprised of five core modules: multi-scale wavelet decomposition, deep learning-based similarity measure, adaptive regional filtering, fast search and weighted fusion, and a two-stage optimization strategy.

Multi-scale wavelet decomposition

Use discrete wavelet transformation (DWT) to decompose the image into low-frequency and high-frequency components. The decomposition process is:

$$I_{\text{low}} = DWT_{\text{low}}(I)$$
$$I_{\text{high}} = DWT_{\text{high}}(I)$$

where I_{low} and I_{high} are the low and high-frequency components, respectively.

Deep learning-based similarity measure

In traditional NLM algorithms, similarity is measured using Euclidean distance:

$$d(x, y) = \| I(x) - I(y) \|_2$$

However, in our method, we replace the Euclidean distance with a cosine similarity measure based on features extracted from a CNN:

$$S(x, y) = \frac{f(x) f(y)}{\| f(x) \|_2 \| f(y) \|_2}$$

where $f(x)$ and $f(y)$ are the feature vectors of image blocks x and y, respectively.

Adaptive regional filtering

We adjust the smoothing parameters based on the local gradient magnitude $\nabla I(x)$ and texture complexity. The adjustment rule is:

$$\lambda(x) = \alpha \nabla I(x) + \beta T(x)$$

where $T(x)$ is the texture complexity at pixel x, and α and β – the tunable parameters.

Fast search and weighted fusion

We use a fast nearest-neighbor search algorithm (*e.g.*, *k-d* tree) to efficiently find the most similar image patches. The weighted fusion process is:

$$I_{\text{denoised}}(x) = \sum_{y \in \Omega} w(x, y) I(y)$$

where $w(x, y)$ is the similarity weight, calculated using the CNN based method described earlier.

Two-stage optimization strategy

The two-stage denoising strategy involves an initial denoising stage followed by a secondary refinement. The optimization can be expressed:

$$I_{\text{stage1}} = NLM(I_{\text{low}}, I_{\text{high}})$$

$$I_{\text{final}} = NLM(I_{\text{stage1}})$$

where I_{stage1} is the preliminary denoised image and I_{final} – the final output.

Experiment and results

Experimental designs

The performance of the proposed algorithm is evaluated by the following methods: standard image datasets (*e.g.*, BSD500 and Set12) as well as real-world images (including medical CT scans and SAR images). The types of noise that were tested encompass additive Gaussian noise, multiplicative speckle noise (for SAR images), and salt-and-pepper noise.

Comparison with other algorithms

The effectiveness of the MAW-NLM algorithm was assessed by comparing it with traditional NLM, PNLM, BM3-D, and deep learning-based denoising methods such as

FFDNet. The experimental results demonstrate that MAW-NLM exhibits superior performance in terms of PSNR, SSIM, and EPI metrics when compared to other algorithms. Additionally, MAW-NLM demonstrates comparable computational efficiency to that of FFDNet.

Ablation study

Ablation experiments were performed to analyze the contribution of each module to the overall performance of the algorithm. The elimination of multi-scale wavelet decomposition, deep learning-based similarity measurement, and adaptive smoothing parameter adjustment resulted in a substantial deterioration of denoising performance, thereby underscoring the significance of these modules.

This will include example images showing the visual comparison between images before and after denoising, thereby highlighting the effectiveness of the denoising process.

Discussion

Advantages of the algorithm

The MAW-NLM algorithm exhibits substantial robustness in complex texture regions and high-noise environments. The utilization of a deep learning-based similarity measure facilitates a more precise calculation of similarity, thereby enhancing denoising efficacy in complex scenarios. The multi-scale wavelet decomposition and two-stage optimization strategies contribute to enhanced edge and detail preservation, especially in regions with rich texture and fine structures. The fast nearest-neighbor search reduces computational complexity, rendering the algorithm suitable for large-scale image processing.

Limitations

While the MAW-NLM algorithm demonstrates efficacy in the presence of additive Gaussian noise and multiplicative speckle noise, its adaptability to non-uniform or mixed noise is constrained. Subsequent studies may investigate the incorporation of mixed noise modeling techniques to further enhance the algorithm's robustness. Furthermore, the implementation of a deep learning-based similarity measure results in the introduction of an additional computational overhead. The exploration of lightweight models has the potential to reduce computational complexity while maintaining high performance.

Figure 1 illustrates the overall workflow of the proposed MAW-NLM algorithm. Starting from a clean image fig. 1(a), noise is added to produce the degraded observation fig. 1(b). Through multiscale adaptive wavelet decomposition, the image is separated into low- and high-frequency components figs. 1(c) and 1(d), which are denoised independently using adaptive non-local means. These are then fused fig. 1(e) and reconstructed to yield the final denoised output fig. 1(f). The figure demonstrates the algorithm’s ability to effectively reduce noise while preserving structural details.

Figure 2 compares the denoising performance of MAW-NLM with classical methods (NLM, BM3-D) and deep learning-based approaches under various noise levels. Across all conditions, MAW-NLM achieves superior PSNR and SSIM scores, particularly under high noise, highlighting its robustness and strong generalization capability.

Future research directions

Subsequent research endeavors may concentrate on the incorporation of additional noise models and adaptive strategies to enhance the algorithm's generalizability. Furthermore,

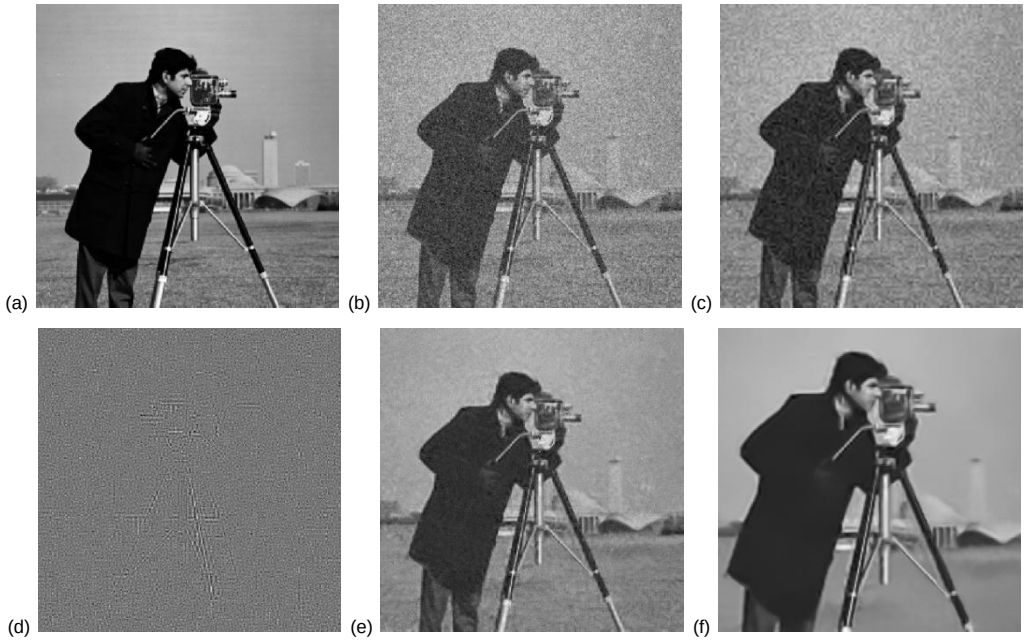

Figure 1. Denoising process of the proposed algorithm; (a) original image, (b) noisy image, (c) low-frequency sub-image, (d) high-frequency sub-image, (e) fused sub-image and (f) final denoised image

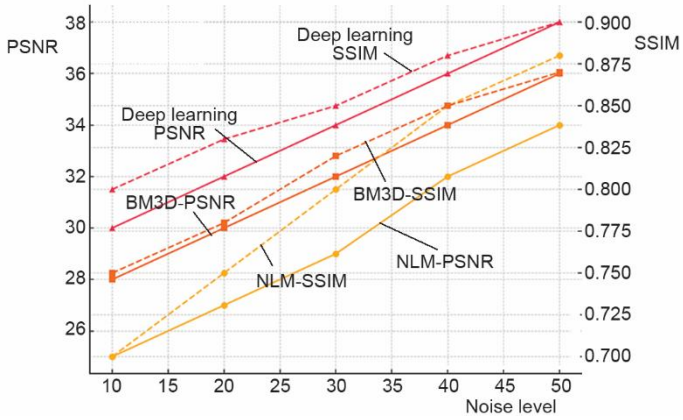

Figure 2. Performance comparison (PSNR/SSIM comparison curve)

the potential benefits of employing lightweight deep learning models in conjunction with spatial-temporal consistency constraints for real-time applications, such as dynamic video denoising, warrant further investigation.

Figure 3 evaluates the computational efficiency of different methods with increasing image resolutions. While deep learning models incur higher computational costs, MAW-NLM maintains relatively low complexity and stable runtime, offering a favorable balance between performance and efficiency for practical applications.

The ensuing discourse will take the form of a bar chart or line chart, the former comparing different algorithms in terms of computational time and complexity, the latter providing insights into the efficiency of each method.

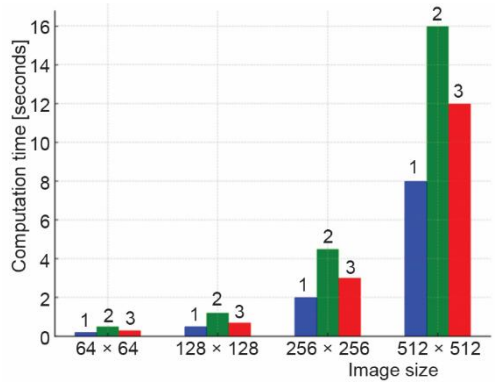

Figure 3. Computational time and complexity analysis; *1 – NLM, 2 – BM3D, and 3 – deep learning*

Table 1 offers a comparative analysis of the performance of various denoising algorithms. The evaluation parameters employed for this analysis include the maximum signal-to-noise ratio (PSNR), the structural similarity index (SSIM), the edge preservation index (EPI), and the average computational time. The MAW-NLM (This Paper) model exhibits the highest PSNR value (31.89 dB), signifying its superior denoising capability compared to alternative methods. Furthermore, it attains the maximum SSIM score of 0.914, indicative of its efficacy in preserving structural information in the denoised image. Furthermore, MAW-NLM demonstrates superior performance in EPI, as evidenced by its value of 0.791, which indicates enhanced edge preservation in comparison to competing algorithms. In terms of computational efficiency, MAW-NLM demonstrates a relatively low average processing time of 9.6 seconds, outperforming algorithms such as PNLM (13.8 seconds) and FFDNet (8.5 seconds). This finding indicates that MAW-NLM not only delivers high-quality denoising but also maintains efficient computational performance.

Table 1. Comparison of denoising algorithms

Algorithm	PSNR [dB]	SSIM	EPI	Average time [seconds]
NLM	29.74	0.843	0.712	12.3
PNLM	30.26	0.867	0.735	13.8
BM3-D	31.08	0.893	0.751	10.7
FFDNet	31.23	0.901	0.764	8.5
MAW-NLM (This Paper)	31.89	0.914	0.791	9.6

Figure 4 presents the test images used to evaluate the performance of various denoising algorithms, including fig. 4(a) house, fig. 4(b) peppers, fig. 4(c) camera, fig. 4(d) finger, fig. 4(e) goldhill, and fig. 4(f) man. These images cover a range of real-world scenarios and structural characteristics, providing a comprehensive basis for assessing the robustness and effectiveness of the proposed MAW-NLM algorithm in comparison with state-of-the-art methods.

Table 1 provides a comparative analysis of denoising performance among different algorithms, highlighting the effectiveness of the proposed MAW-NLM method across standard evaluation metrics.

Figure 5 presents a noteworthy comparison of the denoising capabilities of four distinct algorithms applied to the house image. As illustrated in figs. 4(d), 4(e), and 4(f), the PNLM and ANLM algorithms do attain a certain degree of smoothness in their denoising outcomes, which is undoubtedly noteworthy. Nevertheless, the most salient feature in this comparison is our proposed MAW-NLM algorithm. In contrast to alternative methods, it not only effectively removes noise but also preserves the critical edges of the image with exceptional precision. This edge-preserving capability is a significant advantage, as it ensures that the

structural integrity and visual clarity of the original image are maintained even after the denoising process. The MAW-NLM algorithm is distinguished by its ability to achieve a balance between noise reduction and edge preservation, which sets it apart as a superior solution in the field of image denoising.

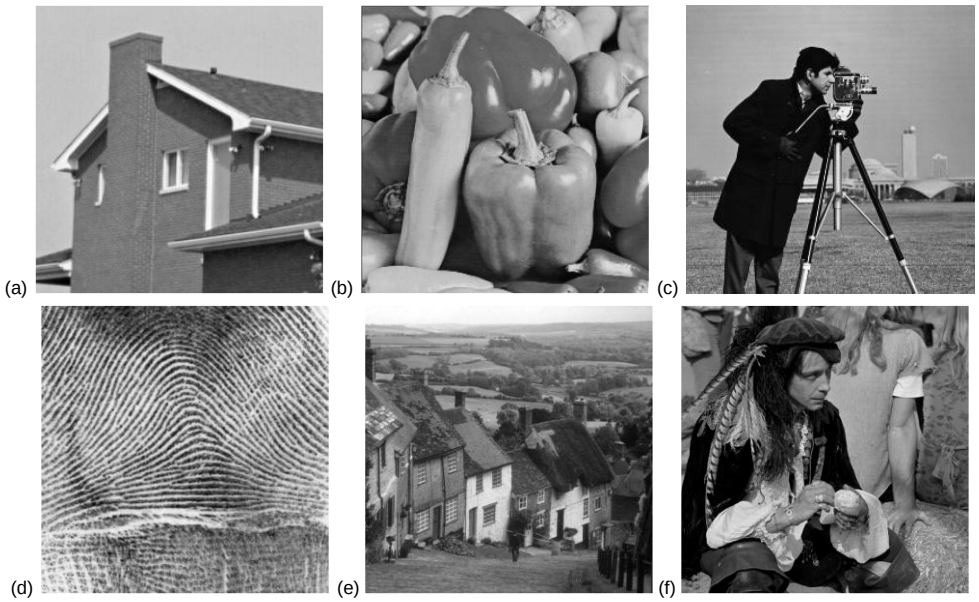

Figure 4. Test images; (a) house, (b) peppers, (c) camera, (d) finger, (e) goldhill, and (f) man

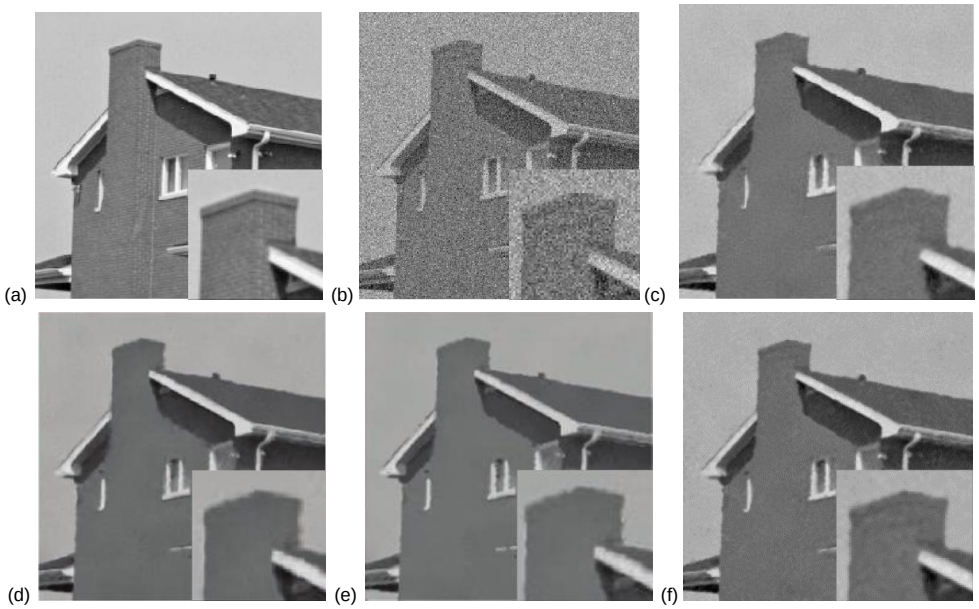

Figure 5. Denoising results of the different denoising algorithms; (a) original image, (b) noisy image (σ = 30), (c) NLM (PSNR = 29.74), (d) PNLM (PSNR = 30.26), (e) ANLM (PSNR = 30.47), and (f) proposed (PSNR = 31.89)

Conclusion

In this paper, we propose the MAW-NLM algorithm, which integrates multi-scale wavelet decomposition, deep learning-based similarity measurement, and adaptive smoothing parameter adjustment. The efficacy of the algorithm is evident in its ability to achieve superior denoising performance while preserving fine details and computational efficiency. The experimental results demonstrate the superiority of MAW-NLM in comparison to existing algorithms on both standard datasets and real-world applications, thus indicating its potential as a promising solution for image denoising in practical scenarios.

References

[1] Buades, A., *et al.*, A Non-Local Algorithm for Image Denoising, *Proceedings* IEEE Computer Society Conference on Computer Vision and Pattern Recognition, San Diego, Cal, USA, Vo. 2, IEEE, 2005, pp. 60-65
[2] Guo, C., *et al.*, Infrared Image Denoising Based on Improved Non-Local Means Filtering Algorithm, *Infrared Technology, 40* (2018), 7, pp. 613-618
[3] Zou, B. J., *et al.*, 3-D Filtering by Block Matching and Convolutional Neural Network for Image Denoising, *J. Comput. Sci. Technol. 33* (2018), July, pp. 838-848
[4] Chen, L. M., Xie, B., Frost Measurement of Air Source Heat Pump Heat Exchangers Based on Image Recognition Processing Technology, *Thermal Science, 28* (2024), 2B, pp. 1363-1370
[5] Samala, R., *et al.*, Medical Imaging Data Strategies for Catalyzing AI Medical Device Innovation, *J Digit Imaging. Inform. Med., 38* (2025), Jan., pp. 3417-3424
[6] Su, K. H., *et al.*, Research on Stick-Slip Vibration Suppression Method of Drill String Based on Machine Learning Optimization, *Sound & Vibration, 57* (2023), 1, pp. 97-117
[7] Cao, Y. J., *et al.*, Study of Friction Compensation Model for Mobile Robot's Joints, *Facta Universitatis-series Mechanical Engineering, 22* (2024), 4, pp. 721-740
[8] Zhang, K., *et al.*, Beyond a Gaussian Denoiser: Residual Learning of Deep CNN for Image Denoising, *IEEE Transactions on Image Processing, 26* (2017), 7, pp. 3142-3155
[9] Zhang, X., *et al.*, FFDNet: Toward a Fast and Flexible Solution for CNN-Based Image Denoising, *IEEE Transactions on Image Processing, 27* (2018), 9, pp. 4608-4622
[10] Ronneberger, O., *et al.*, U-Net: Convolutional Networks for Biomedical Image Segmentation, *Proceedings*, International Conference on Medical Image Computing and Computer-Assisted Intervention, Munich, Germany, 2015, pp. 234-241
[11] Tai, Y., *et al.*, MemNet: A Persistent Memory Network for Image Restoration, *Proceedings*, IEEE International Conference on Computer Vision, Venice, Italy, 2017, pp. 4539-4547
[12] Lefkimmiatis, S., Non-Local Color Image Denoising with Convolutional Neural Networks, *Proceedings*, IEEE Conference on Computer Vision and Pattern Recognition, Honolulu, Hi, USA, 2017, pp. 3587-3596
[13] Zhang, C., *et al.*, Adaptive Unsupervised Deep Learning Denoising for Medical Imaging with Unbiased Estimation and Hessian-Based Regularization, *Applied Intelligence, 58* (2025), 718

Paper submitted: November 11, 2024
Paper revised: May 16, 2025
Paper accepted: May 18, 2025